BOREAS An international journal of Quaternary research

9000 years of changes in peat organic matter composition in Store Mosse (Sweden) traced using FTIR-ATR

ANTONIO MARTÍNEZ CORTIZAS, JENNY K. SJÖSTRÖM, ELEONOR E. RYBERG, MALIN E. KYLANDER, JOERI KAAL, OLALLA LÓPEZ-COSTAS, NOEMI ÁLVAREZ FERNÁNDEZ AND RICHARD BINDLER

BOREAS

Martínez Cortizas, A. Sjöström, J. K., Ryberg, E. E., Kylander, M. E., Kaal, J., López-Costas, O., Álvarez Fernández, N. & Bindler, R.: 9000 years of changes in peat organic matter composition in Store Mosse (Sweden) traced using FTIR-ATR. *Boreas*. https://doi.org/10.1111/bor.12527. ISSN 0300-9483.

Store Mosse (the 'Great Bog' in Swedish) is one of the most extensive bog complexes in southern Sweden (~77 km^2), where pioneering palaeoenvironmental research has been carried out since the early 20th century. This includes, for example, vegetation changes, carbon and nitrogen dynamics, peat decomposition, atmospheric metal pollution, mineral dust deposition, dendrochronology, and tephrochronology. Even though organic matter (OM) represents the bulk of the peat mass and its compositional change has the potential to provide crucial ecological information on bog responses to environmental factors, peat OM molecular composition has not been addressed in detail. Here, a 568-cm-deep peat sequence was studied at high resolution, by attenuated reflectance Fourier-transform infrared spectroscopy (FTIR-ATR) in the mid-infrared region (4000–400 cm^{-1}). Principal components analysis was performed on selected absorbances and change-point modelling was applied to the records to determine the timing of changes. Four components accounted for peat composition: (i) depletion/accumulation of labile (i.e. carbohydrates) and recalcitrant (i.e. lignin and other aromatics, aliphatics, organic acids and some N compounds) compounds, due to peat decomposition; (ii) variations in N compounds and carbohydrates; (iii) residual variation of lignin and organic acids; and (iv) residual variation of aliphatic structures. Peat decomposition showed two main patterns: a long-term trend highly correlated to peat age (r = 0.87), and a short-term trend, which showed five main phases of increased decomposition (at ~8.4–8.1, ~7.0–5.6, ~3.5–3.1, ~2.7–2.1 and ~1.6–1.3 ka) – mostly corresponding to drier climate and its effect on bog hydrology. The high peat accumulation event (~5.6–3.9 ka), described in earlier studies, is characterized by the lowest degree of peat decomposition of the whole record. Given that FTIR-ATR is a quick, non-destructive, cost-effective technique, our results indicate that it can be applied in a systematic way (including multicore studies) to peat research and provide relevant information on the evolution of peatlands.

Antonio Martínez Cortizas (antonio.martinez.cortizas@usc.es) and Noemi Álvarez Fernández, EcoPast, Faculty of Biology, University of Santiago de Compostela, Campus Sur, Santiago de Compostela 15782, Spain; Jenny K. Sjöström, Eleonor E. Ryberg and Malin E. Kylander, Department of Geological Sciences and the Bolin Centre for Climate Research, Stockholm University, Stockholm SE-10691, Sweden; Joeri Kaal, Pyrolyscience, Madrid, Spain and EcoPast, Faculty of Biology, University of Santiago de Compostela, Santiago de Compostela 15782, Spain; Olalla López-Costas, EcoPast, Faculty of Biology, University of Santiago de Compostela, Santiago de Compostela 15782, Spain and Archaeological Research Laboratory, Stockholm University, Wallenberglaboratoriet, Stockholm 10691, Sweden; Richard Bindler, Department of Ecology and Environmental Science, Umeå University, Umeå 901 87, Sweden; *received 15th December 2020, accepted 2nd March 2021.*

Store Mosse (the 'Great Bog') is one of the most extensive bog complexes in southern Sweden (~77 km^2) and a protected national park since 1982. This site's rich scientific history reaches back over 100 years. A detailed map of peat thickness within the basin was produced already in 1912 and Store Mosse first appeared in a scientific publication in 1932 (Granlund 1932). While some studies have explored more recent processes such as soil microbial activity (Robroek *et al.* 2016) and vertical mobility of elements (Hansson *et al.* 2014), the majority of research on Store Mosse has focused on palaeoenvironmental reconstructions, including: vegetation changes (Svensson 1998a, b); metal pollution (Bindler *et al.* 1999, 2003, 2004); carbon and nitrogen dynamics (Malmer *et al.* 1997; Belyea & Malmer 2004; Malmer & Wallen 2004); dendrochronology (Edvardsson *et al.* 2012); decomposition proxies (Hansson *et al.* 2013); mineral dust deposition (Kylander *et al.* 2013, 2016, 2018); and tephrochronology (Wastegård *et al.* 2020).

The strength of Store Mosse as a palaeoarchive lies in its temporal coverage, where at its deepest points (~7 m) it represents 10 ka of history, showing spatially consistent and extensive vegetation shifts and stage transitions (Svensson 1988a). Coring efforts that reach the underlying sand often render sequences with a short basal gyttja section, likely a remnant of Lake Fornbolmen, an ice-dammed lake that existed in the area after deglaciation (~14 000 years ago; Lundqvist & Wohlfarth 2001; Fig. 1). With isostatic uplift Lake Fornbolmen eventually drained, giving way to the development of a fen from ~9.0 ka ago. The transition from the fen to the *Sphagnum*-rich bog occurs sometime between 6.0 and 5.4 ka ago (Svensson 1998a, b; Malmer *et al.* 1997). Perhaps the most intriguing aspect regarding peat accumulation dynamics in Store Mosse is the exceptional high peat accumulation event (HPAE) that occurred from ~5.6 to ~3.9 cal. ka BP (Kylander *et al.* 2013, 2016, 2018). Peat accumulation rates (PAR) and carbon accumulation

DOI 10.1111/bor.12527

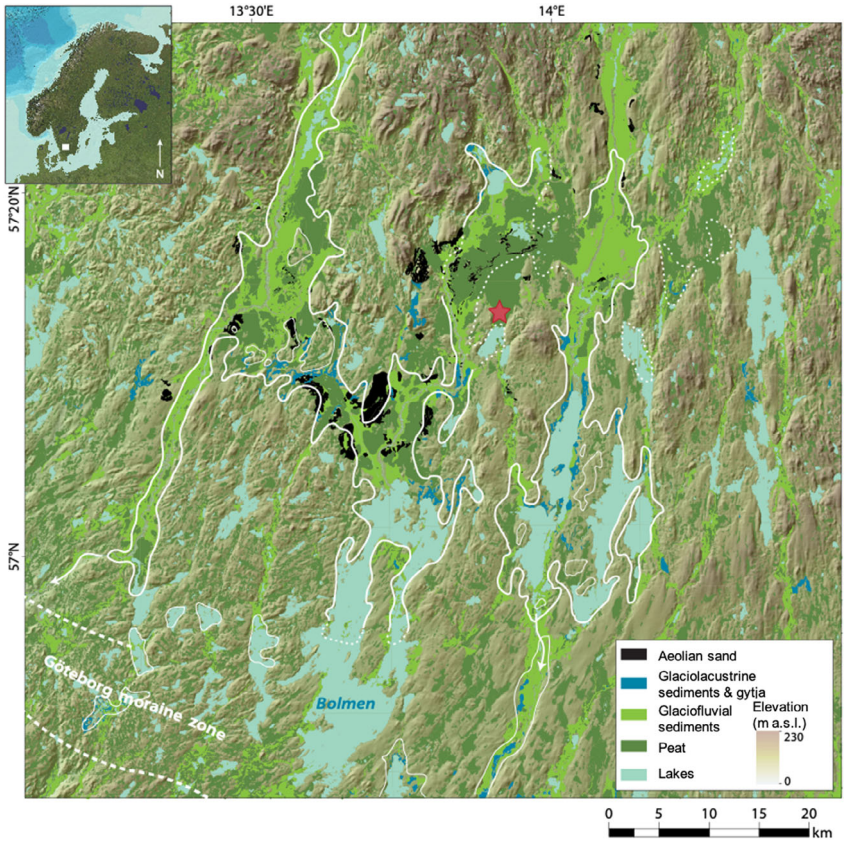

Fig. 1. Location of the Store Mosse bog complex and the sampling site. The white line indicates the modelled area covered by the glacial lake Fornbolmen.

rates (CAR) in this section of the peat sequence are ~2.5-fold higher than those found in a typical ombrotrophic northern peatland (Loisel *et al.* 2014). Recent analyses of a nearby bog indicate this was likely a regional event (Sjöström *et al.* 2020). This HPAE is thought to have been driven by both increased wetness as well as mineral dust fertilization as opposed to a change in vegetation composition (Kylander *et al.* 2018).

Systematic studies of the compounds that constitute the peat organic matter (OM) of the Store Mosse sequence have not yet been performed. The only exceptions are a study of peat decomposition proxies in the uppermost 70 cm (~500 years; Hansson *et al.* 2013) and a pyrolysis-GC-MS study of 20 samples covering the HPAE (Kylander *et al.* 2018). Most of the techniques applied to study peat OM are time-consuming and destructive, causing sample loss. Mid-infrared spectroscopy, however, is efficient in this regard as it needs minimum sample preparation (drying and milling), it is quick (2–3 min per sample), non-destructive, and provides information on the bulk material – avoiding possible artifacts or transformations related to extractions. The downside is that the interpretation of the spectra is complex due to the admixture of compounds present in peat and overlapping vibrations (Stevenson & Goh 1971; Coates 2000; Socrates 2001; Larkin 2011; Simonescu 2012). Some of these issues can be addressed by applying multivariate techniques that allow for the identification of the main spectral signals and trends in compositional change (Holmgren & Nordén 1988; Chang *et al.* 2001; Chapman *et al.* 2001; Janik *et al.* 2007; Viscarra Rossel & Behrens 2010; Estracanholli *et al.* 2012; Fernández-Getino *et al.* 2013; Biester *et al.* 2014), but, to date, this approach is rarely applied.

Mid-infrared spectroscopy has been extensively applied in soil and peat OM studies for the identification of OM structural types (Senesi *et al.* 1991; Niemeyer *et al.* 1992; Kalbitz *et al.* 1999; Chapman *et al.* 2001; Cocozza *et al.* 2003; Ellerbrock & Gerke 2004; Artz *et al.* 2006, 2008; Zaccone *et al.* 2007; Broder *et al.* 2012; Biester *et al.* 2014; Heller *et al.* 2015; Silva-Sánchez *et al.* 2015), to evaluate litter and peat decomposition (Holmgren & Nordén 1988; Niemeyer *et al.* 1992; Haberhauer *et al.* 1998, 2000; Haberhauer & Gerzabek, 1999; Broder *et al.* 2012; Biester *et al.* 2014; Silva-Sánchez *et al.* 2016) and model trace element accumulation (Pérez-Rodríguez *et al.* 2016). Most of these investigations deal with a quite limited number of samples and are usually paired with other techniques (^{13}C NMR, ESR, Rock-Eval Pyrolysis, Pyrolysis-GC-MS, etc.). Only a handful of papers deal

with peat sequences subsampled with higher resolution (Cocozza *et al.* 2003; Zaccone *et al.* 2007, 2011; Krumins *et al.* 2012; Silamikele *et al.* 2012; Biester *et al.* 2014), but these studies focused on the upper metre or less of the peat deposit and seldom on long-term environmental reconstructions (Bourdon *et al.* 2000). Since many peatlands, as Store Mosse, started to form at the beginning of the Holocene or even earlier, there is a wide range of potential factors (e.g. time, climate changes, vegetation changes, land-use changes) that might have contributed to or affected the peat OM composition. Thus, changes in peat OM composition potentially contain crucial ecological information on the bog responses to environmental factors. Long, high-resolution records are necessary to evaluate the weight of these factors through time.

Store Mosse is an ideal peatland for a systematic study of the molecular composition of peat because there is a wealth of high-resolution data available from previous studies and the accumulated peat covers almost the whole Holocene period with distinctive evolutionary phases (gyttja rich lake sediments, fen, and the transition to bog). By analysing a long core (568 cm, ~10 ka), we aim at both establishing a robust methodological approach to treat (Álvarez Fernández & Martínez Cortizas 2020) and extract (using multivariate statistical analysis) information from the spectral properties of the peat, and to decipher the ecological factors that were involved in the reconstructed changes. Specifically, the objectives of this research are to: (i) characterize OM functionalities by attenuated reflectance Fourier-transform infrared spectroscopy (FTIR-ATR), (ii) determine the main OM compounds and their variation with depth/age, (iii) compare the FTIR-ATR generated data with available pyrolysis OM data for the HPAE, and (iv) establish the timing of compositional changes and, thus, how the bog responded to Holocene environmental drivers.

Material and methods

Location and sampling

Store Mosse National Park (160–170 m a.s.l.) is located in south-central Sweden in the County of Jönköping, at the southern edge of the Southern Swedish Highlands (Fig. 1). The peatland slopes slightly to the south, which is consequently the oldest and thickest section of the bog; visible hummock strings run perpendicular to this slope. The present bog surface is dominated by *Sphagnum* mosses with many areas co-dominated by graminoids (*Eriophorum vaginatum* L., *Tricophorum cespistosum* L. and *Rhynchospora alba* L.), and ericaceous dwarf shrubs (*Calluna vulgaris* (L.) Hull, *Vaccinium oxycoccos* L. *Erica tetralis* L. and *Empetrum nigrum* L.). *Drosera* spp. and lichens (mostly *Cladonia* spp.) also occur extensively. There are extensive glacial deposits in the area, which were reworked through aeolian processes, resulting in a dune system that bisects Store Mosse, which was emplaced ~8 to ~6 ka (Bjermo 2019). The climate is maritime with relatively cool summers and mild winters. The annual average temperature is 5.5 °C and the average precipitation is 800 mm year^{-1} (SMHI 2009).

A complete peat sequence was collected from the southern bog part of the peatland complex (latitude 57°13′37″N, longitude 13°55′17″E) in November 2008 using a Russian corer (1 m in length, ø 7.5 cm). Eight sections were collected with 25-cm overlap taken in two adjacent holes. Cores were frozen and with a stainless-steel knife cut into 1-cm slices, which were freeze-dried and weighed. Bulk density was then calculated and used to align the overlapping cores for a composite sequence of 568 cm. Samples were milled with a plant mill equipped with Teflon vials and agate milling balls.

Previous available data

Full details of the 19 macrofossil age dates used to build the chronology of the sequence are given in Kylander *et al.* (2013). For the present research we constructed an updated age model (Fig. S1) using Bacon version 2.2 (Blaauw & Christen 2011), developed specifically to improve estimation of peat accumulation rates (PAR) and age uncertainties, replacing the previous CLAM version (Kylander *et al.* 2013, 2016, 2018). Previously published PAR, ash content, C, N, C/N and degree of peat humification (DPH) are presented in Fig. S2 – using this updated age depth model. The PAR are rather typical for ombrotrophic systems with baseline values around 40 to 50 g m^{-2} a^{-1} (Loisel *et al.* 2014). The exception to this is the HPAE, which increases from background values at 439 cm (~5.51 cal. ka BP), with maxima (~2.5-fold higher) occurring between 412–348 cm (~5.24–4.79 cal. ka BP), and a return to background values by 289 cm (~3.95 cal. ka BP). Ash contents are initially around 13% and steadily decrease until 552 cm (~8.70 cal. ka BP), remaining below 2% to the top of the sequence. The higher ash content in the basal section likely represents the lake stage and the infilling of the basin. The fen–bog transition occurs at 443 cm (~5.6 cal. ka BP). In general, C is low in the lake stage, higher in the fen and lower again in the HPAE, while the bog stage shows oscillating values. Nitrogen decreases from the lake stage through the fen, reaching profile lows in the HPAE and showing variability relative to C in the bog section. The largest C/N values (up to 100) are found in the peat section representing the HPAE, in which they are roughly double those seen in all other parts of the sequence. Lastly, the DPH is low in the lake and higher in the fen stages. Again, the HPAE stands out having by far the least decomposed material of the sequence. Similar to the profiles for C and N, the DPH shows an oscillating pattern in the rest of the bog section.

FTIR-ATR analyses

A total of 105 samples (every ~5 cm) were analysed using attenuated reflectance Fourier-transform infrared spectroscopy (FTIR-ATR). FTIR-ATR spectra were acquired at 4 cm^{-1} resolution in the mid-infrared (MIR) region 4000–400 cm^{-1}, by averaging 200 scans, with a Gladi-ATR (Pike Technologies) spectrometer at the IR-Raman facility of the RIAIDT of the Universidade de Santiago de Compostela, Spain. Spectra were baseline corrected in order to avoid bias in the spectroscopic signal due to scattering, reflection, temperature, concentration or instrument anomalies (Griffiths & De Haseth 2007). The average, standard deviation and second derivative spectra were calculated and peak identification (based on the second derivative spectrum) was performed using the {*andurinha*} R (R Core Team, 2020). package (Álvarez Fernández & Martínez Cortizas 2020). Assignment of compounds related to vibrations and classes is based on literature (see references in Table S1), taking into account the limitations imposed on IR interpretation of complex samples (Coates 2000; Socrates 2001; Larkin 2011; Simonescu 2012).

We selected a number of IR ratios to determine relative changes in functional groups/OM compounds with depth/age and type of peat: labile vs. resistant OM (IR_1 and IR_2), aliphaticity (IR_3 and IR_4), short length/branched aliphatics (IR_5), O-rich compounds (IR_6), aromaticity (IR_7) and guaiacyl/syringyl lignin (IR_8). For details, see Data S1.

In the following text, polysaccharides refer to typical FTIR absorbances and pyrolysis products of carbohydrates. Aliphatics are polymethylene chain compounds, i.e. long CH_2 chains with terminal CH_3, although short C-chains such as those in lignin may generate some of the corresponding IR signal as well. Aromatics refer to phenolic and non-phenolic aryl compounds. Guaiacyl (G) and syringyl (S) groups are the main units in lignin, in addition to *p*-hydroxyphenyl.

Statistical methods

We applied principal component analysis (PCA) to the selected MIR vibrations (e.g. Estracanholli *et al.* 2012). All spectra were first standardized using Z-scores, and the PCA performed on the correlation matrix using a varimax rotation, a solution that maximizes the loadings of the variables on the components. This rotation usually provides clearer patterns, helping to identify the underlying (latent) factors affecting peat composition. The fractionation of the communalities is depicted in a simple but informative cumulative graph (see Fig. S3 and Data S1). We also performed a PCA on the molecular data (Py-GC-MS) of the HPAE to extract the main compositional signals and compare them to the FTIR-ATR signals.

To determine whether a variable (vibrations and FTIR ratios in this case) is a good proxy for the underlying process or peat compound captured by a principal component, we used a modification of the selectivity ratio proposed by Rajalahti *et al.* (2009) and utilized, for example, by Muller *et al.* (2014) in FTIR mineral data. Values were linearized by applying logarithm and a proxy value (pV) of 0.5 or greater is considered to identify highly influential vibrations (~log (3), 3 being the reference for selectivity ratios; Rajalahti *et al.* 2009; Muller *et al.* 2014). For details see Data S1.

To objectively evaluate when significant changes occurred in the score records of the extracted components, their probability was assessed using the change-point modelling (CP) routine (Gallagher *et al.* 2011), which was applied in previous investigations on peat records (e.g. Hansson *et al.* 2013; Kylander *et al.* 2013). Iterations (burn-in and burn-out) were set to 10 000. For details see Data S1.

Results

Spectral signal

The absorbance spectra of the peat samples, as well as the standard deviation and average second derivative spectra are depicted in Fig. 2. The spectra are typical of peat material, with high absorption in the wavenumber regions 3400–3200, 3000–2800 and 1800–800 cm^{-1}. These absorptions are characteristic of functional groups in polysaccharides, aliphatics, lignin and other aromatics, organic acids (compounds carrying C=O in acidic groups such as carboxylates), and OH vibrations (from polysaccharides, water and clays) (Cocozza *et al.* 2003; Zaccone *et al.* 2007; Artz *et al.* 2008; Neves Fernandes *et al.* 2010; Krumins *et al.* 2012; Silamikele *et al.* 2012; Klavins & Purnalis 2014; Heller *et al.* 2015; and references in Table S1). Lower absorbance was recorded in the 800–400 cm^{-1} region, likely corresponding to carbohydrates, lignin and minerals (mostly silicates). Low absorbance was also found in the 2200–1900 cm^{-1} region, mostly associated with C (alkynes) and N compounds (aliphatic CN and tertiary amines; Coates 2000; Asapo & Coles 2012), but also with overtones of the 1200–1000 cm^{-1} region (of the polysaccharides; Coates 2000). Very low absorbance was observed in most samples in the 3700–3600 cm^{-1} region, which is associated with clay minerals (Artz *et al.* 2008; Muller *et al.* 2014). The standard deviation spectrum indicates that there are relatively large differences between samples in the regions 3400–3200, 2980–2800, 1750–1350, 1300–1130 and 1100–900 cm^{-1}, and moderate to low variability in 2200–1900 and 800–400 cm^{-1}. The second derivative enabled the identification of close to 100 vibrations; the wavenumbers and their correspondence with functionalities and peat compounds can be found in Table S1.

Figure 3 shows the average spectra of the two main peat stages (i.e. fen and bog) and the HPAE. The HPAE

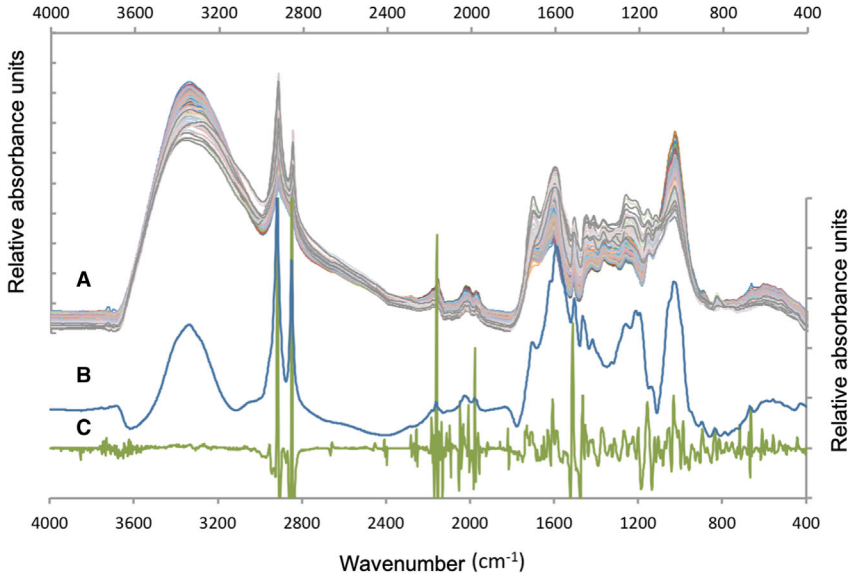

Fig. 2. A. Spectra of the peat samples. B. Standard deviation spectrum (blue line). C. Average second derivative spectrum (reversed; green line) of Store Mosse peat samples.

and post-HPAE bog spectra are almost identical, except for slightly lower absorbances at 1100–900, 1700–1760 and 3300–3200 cm^{-1}, and slightly higher absorbance at 1590–1192 cm^{-1} (Fig. 3A, C) during the HPAE. The fen spectrum is characterized by lower absorptions at 1100–900 and 3400–3200 cm^{-1}, but higher absorptions at 1800–1200 and the 3000–2800 cm^{-1} regions (Fig. 3A, C). More detailed information is provided by the standard deviation spectra (Fig. 3B): the bog peat shows higher variability in comparison to the other two sections, at 1000–900, 1464, 1600–1550, 2030–1960, 2190–2160 and 3400–

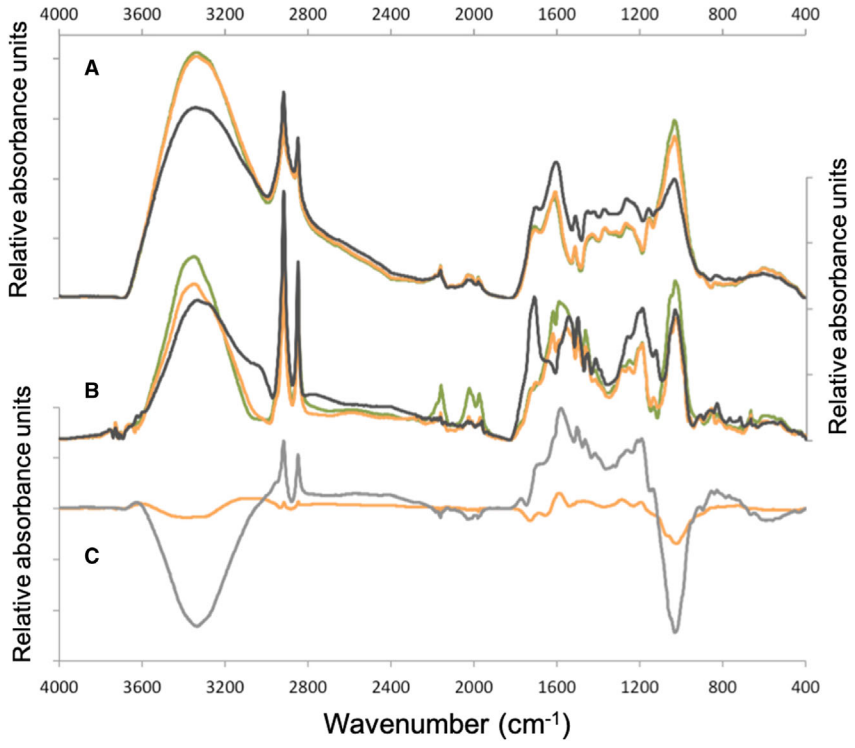

Fig. 3. A. Average spectra of fen peat (black), HPAE peat (orange) and post-HPAE bog peat (green). B. Standard deviation spectra (same colours). C. Difference spectra compared to post-HPAE bog peat: fen minus bog (grey) and HPAE minus post-HPAE bog (orange).

3200 cm^{-1}; the HPAE peat shows similar or slightly lower variability than the rest of the bog peat; while the fen peat shows higher variability at 1300–1100, 1800–1660, 3000–2800 and around 3030 cm^{-1}.

FTIR ratios

The depth distributions of the IR ratios are depicted in Fig. 4. IR_1 and IR_2 (both representing the relationship between labile and resistant OM) are highly and positively correlated (r = 0.97) and moderately correlated (r = 0.51–0.62) with IR_6 (O-rich compounds), but negatively correlated with IR_4 (aliphaticity; r = −0.91), IR_5 (short length/branched aliphatics; r = −0.66), IR_7 (aromaticity; r = −0.77) and IR_8 (guaiacyl/syringyl lignin; r = −0.64) (Table S2). IR_1 and IR_2 show lower values in the fen section (below 416 cm) and higher in the bog section (above 416 cm) (Fig. 4). IR_4, IR_5 and IR_8 show, essentially, the opposite pattern. IR_4 and IR_5 have the same distribution in the bog section but decouple in the fen section. IR_3 (aliphaticity) values decrease slightly with depth in the bog section and more rapidly in the fen. IR_6 also decreases slightly in the bog section, but values in the fen section are higher until 515 cm and then decrease abruptly. IR_7 slowly increases with depth in the bog and almost exponentially in the fen section.

Principal component analysis

The PCA resulted in five components (53, 19, 10, 8 and 4% of the variance, respectively) that explain 91% of the total spectral variance. Almost all variables

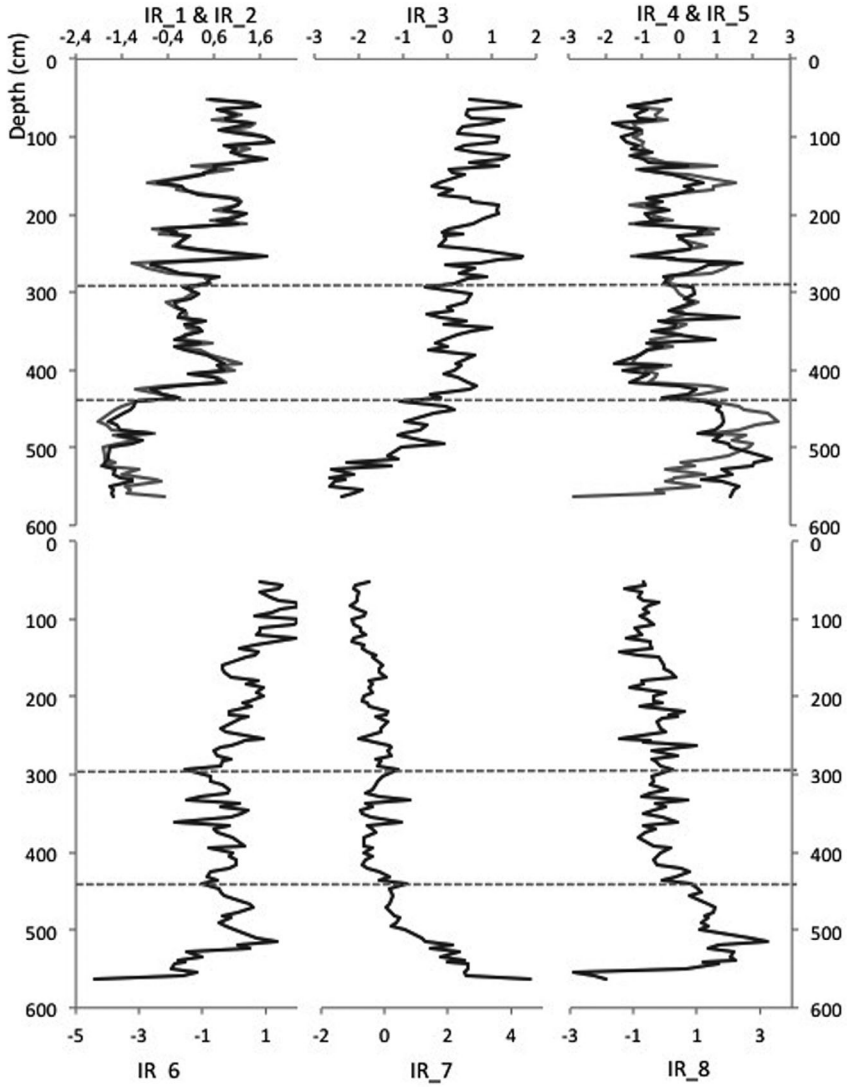

Fig. 4. Depth records of the FTIR ratios (z-scores) in the Store Mosse core. The dashed lines indicate the upper limit of the fen section (lower line) and the upper limit of the HPAE (upper line). IR_1: black line and IR_2: grey line; IR_4: black line and IR_5: grey line.

showed large (>0.8) communalities. The first component, $_{IR}$Cp1 shows large (>0.7) positive loadings (Table S1) for vibrations of lignin and other aromatics (1628–1223, 835, 754 cm^{-1}), organic acids (2569, 1709 and 1676 cm^{-1}), aliphatics (2918, 2850, 874, 771, 719 cm^{-1}), carbohydrates (1157 and 783 cm^{-1}) and proteinaceous compounds (amide I and amide II, 1628 and 1552 cm^{-1}). Some vibrations can also correspond to mineral matter, particularly silicates (814 and 783 cm^{-1}) and carbonates (874 cm^{-1}). Vibrations corresponding to lignin (1628–754 cm^{-1}), aliphatics (771 cm^{-1}), and minor carbohydrate bands (1201 and 783 cm^{-1}) with positive loadings, and the main vibrations corresponding to carbohydrates/polysaccharides (1072–900 cm^{-1}; plus 592–528 cm^{-1}, also associated with minerals), OH vibrations (3400–3280 cm^{-1}) and proteinaceous compounds (1655 and 1552 cm^{-1}), with negative loadings, show large pV (>0.5) and can be considered good proxies for the underlying factor in $_{IR}$Cp1 (Fig. 5).

Vibrations characteristic of aliphatic groups (2956, 2918, 2871, 2850, 874, 719 cm^{-1}), carbohydrates (1157 and 1107 cm^{-1}; also 467–417 cm^{-1} of carbohydrates+minerals) and organic acids show low pV for $_{IR}$Cp1 (Fig. 5). These vibrations correspond to compounds with more complex distributions and which are affected by more than one factor, i.e. the process reflected by $_{IR}$Cp1 is not the only one affecting their distribution in the peat. $_{IR}$Cp1 shows an inverse correlation with IR_1, IR_2, IR_3 and IR_6, and is directly correlated with IR_4, IR_7, IR_5 and IR_8 (Table 1).

The second principal component, $_{IR}$Cp2, shows large positive loadings for vibrations in the region 2241–1944 cm^{-1}, which may correspond to alkynes/N compounds and overtones of polysaccharides (1200–1000 cm^{-1}) (Table S1). The 1944 cm^{-1} vibration and those in the region 2065–2214 cm^{-1} have large pV, while the regions 2050–1954 and 2241–2231 cm^{-1} have low pV (Fig. 5). Vibrations on these latter regions have part of their variances in $_{IR}$Cp1 (negative and positive loadings, respectively; Fig. S2). $_{IR}$Cp2 does not show relevant correlations to any of the IR ratios (Table 1).

The third component, $_{IR}$Cp3, is represented by vibrations related to lignin (1124 cm^{-1}) and organic acids (1766 and 1734 cm^{-1}) (positive) and to vibrations corresponding to proteinaceous compounds (3107–3005 cm^{-1}, amide A and B) (negative) (Table S1). Only two of the proteinaceous vibrations (Fig. 5) have large pV. $_{IR}$Cp3 shows a moderate, positive, correlation with IR_6 (Table 1).

The fourth component, $_{IR}$Cp4, includes variance of vibrations at 964–895 cm^{-1} (positive) and in the region 3700–3600 cm^{-1} (negative) (Table S1, Fig. S3). Positive loadings may be related to vibrations of both minerals (i.e. silicates) and carbohydrates, while negative loadings correspond to vibrations that can be assigned to clay minerals. Only two of the vibrations (3614 and 3602 cm^{-1}) have large pV (Fig. 5). $_{IR}$Cp4 does not show relevant correlations to any of the IR ratios or peat properties (Table 1), but rather seems to mainly be related to the inorganic mineral fraction and will not be further discussed here.

The fifth component, $_{IR}$Cp5, includes part of the variance of aliphatic vibrations (2918–2850 cm^{-1}, negative loadings) and of the 592–417 cm^{-1} region (positive), which may correspond to carbohydrate and mineral vibrations (Table S1, Fig. S3), all of which have low pV. $_{IR}$Cp5 shows negative, moderate, correlations with IR_5 (Table 1).

The IR ratios were also included in the $_{IR}$PCA to check their ability to reflect the changes in peat OM in Store Mosse. For most of them (IR_1, IR_2, IR_3, IR_4 and IR_7) their variance was primarily allocated into $_{IR}$Cp1 (Table S1, Fig. S3). The variances of the others are mainly split between two (IR_6, IR_8) or three (IR_5) components (Fig. S3). Only IR_1, IR_2 and IR_4 have large pV, all for $_{IR}$Cp1 (Fig. 5).

Depth records of the changes in peat organic matter composition

The scores record of the first principal component ($_{IR}$Cp1) is the only one that shows an increase with depth/age (r = 0.87), which is low to moderate in the bog section and more intense in the fen section (Fig. 6). The time-detrended first component scores, d_{IR}Cp1, show a similar pattern to $_{IR}$Cp5, which is related to aliphaticity, with peaks at 159, 219, 262, 333, 361, 466 and 519 cm depth (Fig. 6). $_{IR}$Cp2 shows two main sections with high ratios, during the HPAE (294–405 cm) and in the upper 140 cm. At the bottom (>540 cm) values are also relatively high. $_{IR}$Cp3 shows decreasing values (i.e. decrease in organic acids and increase in proteinaceous compounds; correlation to age r = −0.87) in the bog section, a rapid increase in the fen and an abrupt decrease at the base (>540 cm) of the core.

Correlation between FTIR and peat OM molecular composition in the HPAE section

The PCA on the molecular compositional data (Py-GC-MS) for a restricted set of samples spanning the HPAE section (Kylander *et al.* 2018) provided seven principal components (Table S3), of which the first three aid in the interpretation of the spectral data obtained by FTIR-ATR. The first component, $_{PY}$Cp1, reflects the content of alkanes and alkenes with short and intermediate chain length (C_{16}–C_{26}) vs. the content of polysaccharides, 4-vinylphenol, 4-isopropenylphenol and other (non-methoxy) phenols, which represent selective

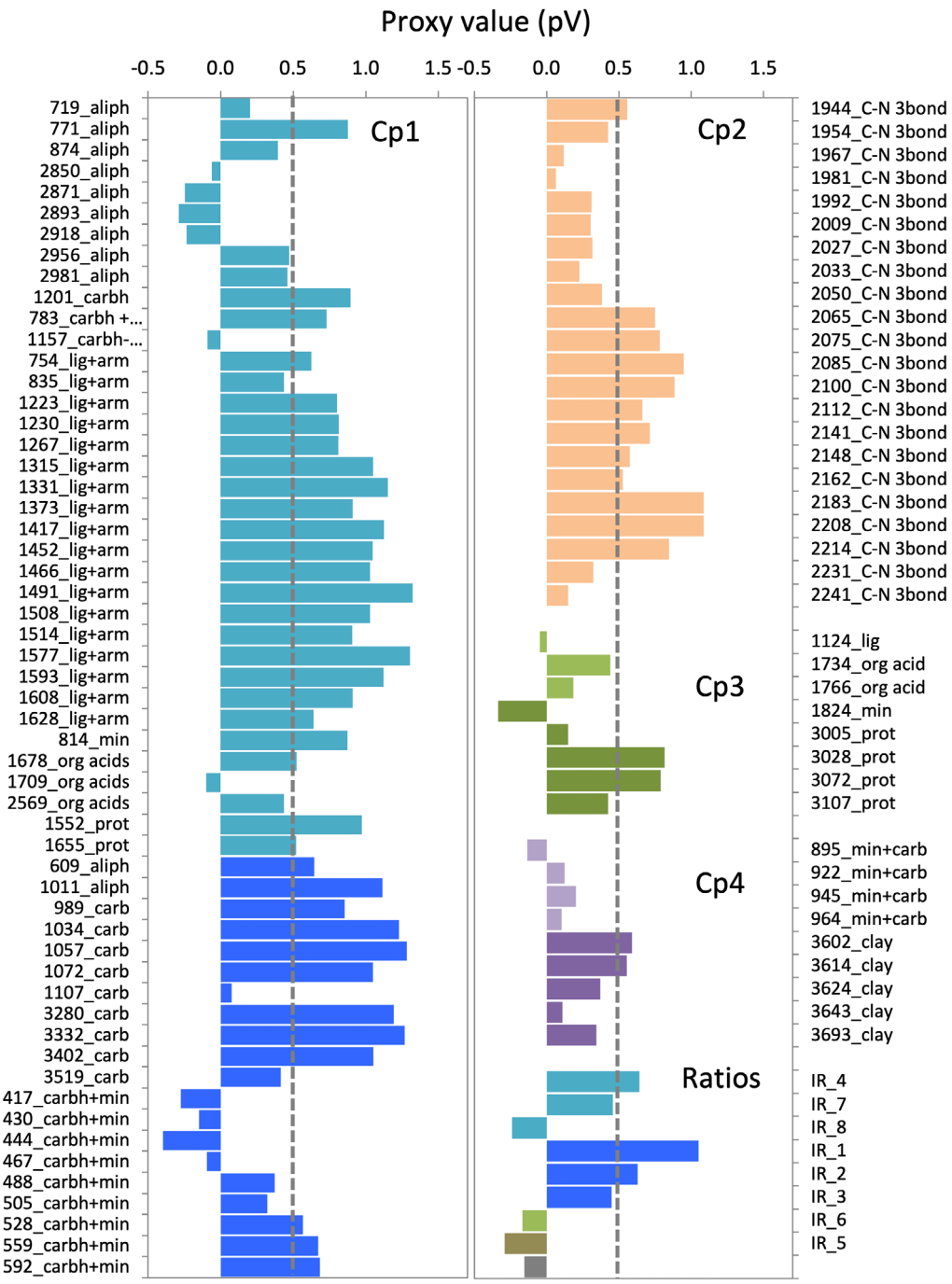

Fig. 5. Proxy values (pV) of the FTIR-ATR vibrations and FTIR ratios. Vibrations are ordered by the component to which the largest proportion of the variance is allocated. The different colours of the bars in the same component correspond to peaks with positive (lighter) or negative (darker) loadings. The dashed line indicates the reference pV for highly influential variables. Cp5 is not represented as it only accounts for minor amounts of the variance of aliphatic and carbohydrates (see Table S1).

degradation of labile phenolic and carbohydrate materials (from graminoids and mosses) and preservation of relatively recalcitrant aliphatic OM. $_{PY}$Cp2 reflects changes in the balance between lignin (guaiacol and syringol moieties, and catechol) and recalcitrant aliphatic and perhaps some microbial OM (alkanes, alkenes, toluene). $_{PY}$Cp3 mainly reflects the depletion of long C-chain alkanes and alkenes (C_{30}–C_{33}; probably from epicuticular waxes) vs. C_{25} methylketone.

The FTIR-PCA components show significant correlations with the pyrolysis components (Table 2) for the HPAE: $_{IR}$Cp1 and $_{IR}$Cp3 are positively correlated and

$_{IR}$Cp5 negatively correlated to $_{PY}$Cp1; $_{IR}$Cp2 is moderately correlated to $_{PY}$Cp2 and $_{PY}$Cp3.

Discussion

Interpretation of the spectral signals of the peat organic matter

From the results described above, we interpret $_{IR}$Cp1 as indicating the enrichment in resistant OM moieties (such as lignin (polyphenols), aliphatics, organic acids and proteinaceous compounds) as the labile compounds (polysaccharides and other labile OM constituents) are depleted. The Py-GC-MS results, restricted to the HPAE, support the interpretation of the IR results as $_{PY}$Cp1 also represents the depletion of labile OM (i.e. polysaccharides) accompanied by an increase in recalcitrant OM (i.e. aliphatics) (Buurman *et al.* 2006; Kaal *et al.* 2007; Biester *et al.* 2014; Schellekens *et al.* 2015; Kylander *et al.* 2018); in addition, $_{IR}$Cp1 is also highly correlated to $_{PY}$Cp1 (Table 2). 4-isopropenylphenol is a marker of sphagnum acid in mosses and, together with 4-vinylphenol (from graminoids and mosses) and primary polysaccharides, is known to be relatively easily degraded (Schellekens *et al.* 2015). $_{IR}$Cp1 thus reflects peat decomposition and seems to respond to a long-term trend (Fig. 6), supported by its high correlation to age, and to shorter-term trends, possibly related to the conditions (mainly bog surface wetness) when the peat was at the surface of the bog (d_{IR}Cp1; Fig. 6). The results of the $_{IR}$PCA are similar to those obtained in a recent FTIR study of peatlands distributed along a transect from the Arctic to the tropics (Hodgkins *et al.* 2018). In this study, the first PCA component showed large negative loadings for carbohydrates and large positive loadings for lignin and other aromatics. In short, our FTIR and Py-GC-MS data are in line with the FTIR results obtained by Hodgkins *et al.* (2018), regarding the effects of decay on polysaccharides and labile phenolic OM (preferentially lost) and the polymethylene aliphatic structures (selectively preserved).

The main difference between the FTIR signal ($_{IR}$PCA) and the OM molecular composition ($_{PY}$PCA) is that the resistant OM signal in $_{IR}$Cp1 is dominated by lignin (high pV, Fig. 5), while in $_{PY}$Cp1 it is dominated by aliphatics. This agrees with previous investigations on the molecular composition of peat OM (Biester *et al.* 2014; Schellekens *et al.* 2015) and can be attributed to the fact that the FTIR and Py-GC-MS data reflect different processes. In these investigations, it was assumed that FTIR better reflects processes related to mass loss (i.e. mineralization) while the more specific pyrolysis data reflect peat decomposition and vegetation change. The complexity of the FTIR spectra and the effect of overlapping absorbances of different functional groups have also been argued as reasons for their 'ambiguity' when compared to Py-GC-MS (Biester *et al.* 2014). An important aspect to consider when interpreting the results of multivariate statistical analyses, such as PCA, is that FTIR produces more information on lignin (and other aromatics) functionalities while Py-GC-MS produces numerous aliphatic compounds in homologous series of *n*-alkanes and *n*-alkenes, generating bias in terms of variance towards the latter because the extraction of the principal components is based on covariation. It is likely that each technique introduces some degree of bias, with non-rotated solutions in particular, depending on which compounds are more represented (i.e. numerous). Nevertheless, each technique produces consistent results in itself and ours are in line with previous investigations of peat using FTIR (Tfaily *et al.* 2014; Hodgkins *et al.* 2018).

The $_{PY}$PCA lignin (guaiacol and syringol moieties) signal allocated to $_{PY}$Cp2 correlates with $_{IR}$Cp2, which shows elevated values at the end of the HPAE. This indicates that, apart from the functionalities already mentioned (alkynes/N compounds), overtones of the lignin vibrations in the region 1200–1100 cm^{-1} also contribute to $_{IR}$Cp2. Furthermore, $_{IR}$Cp2 is also correlated to $_{PY}$Cp3, and it is thus likely affected by the abundance in C_{25} methylketone and the depletion of long-chain *n*-alkane and *n*-alkenes (C_{30}–C_{33}), a triterpenoid and a syringol (i.e. lignin). At the same time, the low pV of the 2050–1940 cm^{-1} region and its partial allocation to $_{IR}$Cp1 (negative, moderate loadings in this component) indicate that $_{IR}$Cp2 also captures the signal of overtones of the 1030–950 cm^{-1} region, which is typical of polysaccharides. $_{IR}$Cp2 may be driven by both increases in alkynes/N compounds, lignin and polysaccharides under enhanced bioproductivity in the mire; for

Table 1. Correlation between the FTIR principal components and the FTIR ratios (dIRCp1: time-detrended first principal component).

	IR_1	IR_2	IR_3	IR_4	IR_5	IR_6	IR_7	IR_8
$_{IR}$Cp1	−0.96	−0.90	−0.86	0.90	0.52	−0.56	0.86	0.60
$_{IR}$Cp2	0.15	0.20	0.10	−0.19	−0.29	0.20	−0.10	−0.30
$_{IR}$Cp3	0.04	−0.09	0.16	0.11	0.41	0.64	−0.30	0.47
$_{IR}$Cp4	0.08	0.08	0.10	0.09	−0.06	0.02	0.10	−0.22
$_{IR}$Cp5	0.17	0.34	−0.33	−0.11	−0.58	−0.06	0.33	0.00
d_{IR}Cp1	−0.50	−0.56	−0.22	0.59	0.57	−0.16	0.25	0.30

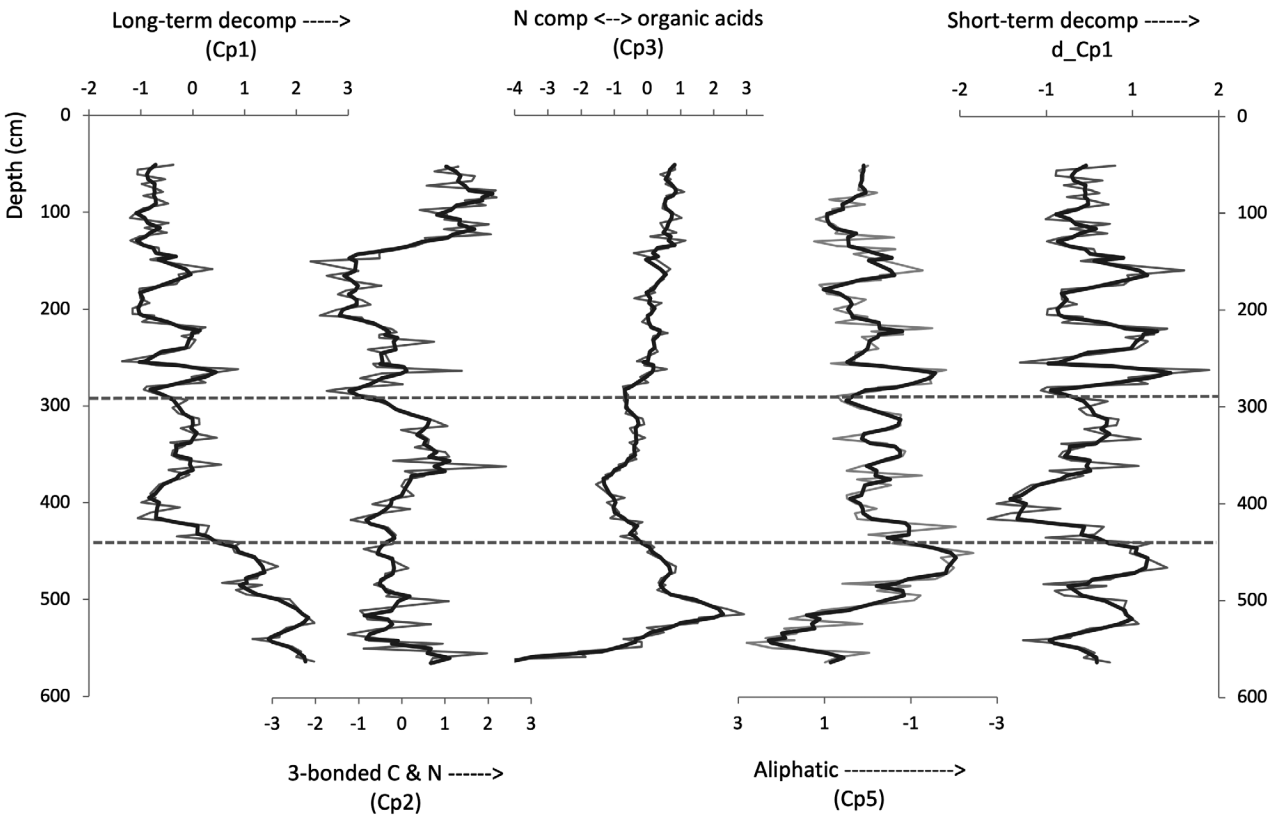

Fig. 6. Depth records of scores of the extracted principal components. The grey line is the actual data and the black line corresponds to the running average. The dashed lines indicate the upper limit of the fen section (lower line) and the upper limit of the HPAE (upper line).

example, high $_{IR}$Cp2 scores are found at the inception of peat accumulation, during the HPAE and at the top of the core. We therefore interpret $_{IR}$Cp2 as reflecting periods of intense shifts in the balance between peat growth and peat decomposition in favour of the first, stimulated by a boost in bioproductivity.

$_{IR}$Cp3 reflects the distribution of proteinaceous compounds (mostly amide A and B vibrations, negative loadings) and part of the variation of the organic acids/carboxylates (positive loadings) (Table S1). This component essentially reflects the distribution of proteinaceous compounds, as suggested by their large pV. A small part of the signal of the organic acids is allocated into $_{IR}$Cp1 (positive loading), indicating that they tend to increase during peat decomposition (Cocozza *et al.* 2003; Zaccone *et al.* 2007, 2011). In the HPAE this component is correlated to $_{PY}$Cp1, which also reflects peat decomposition.

$_{IR}$Cp5 accounts for part of the distribution of aliphatic vibrations (Table S1). Aliphatics are thus allocated to two different components (even three, Table S1 and Fig. S2). While aromatics have been considered active in peat humification (i.e. they can inhibit decomposition; Dommain *et al.* 2011), some studies (Bader *et al.* 2017; Hodgkins *et al.* 2018) conclude that the increase in aliphatics is mainly a relative concentration effect due to the progressive loss of more-labile OM. The scores of this component show a quite similar depth distribution to that of the short-term decomposition signal (d_{IR}Cp1 in Fig. 6) and have no time or bog/fen dependence. This supports the idea that the enrichment in aliphatics is indeed a residual effect due to their lower biodegradability and not to active participation in peat humification (Hodgkins *et al.* 2018).

Most of the IR ratios (IR_1 to IR_4 and IR_7) load significantly in $_{IR}$Cp1 (Table S1), i.e. they mostly reflect peat decomposition. On the one hand, IR_1 and IR_2 (labile/resistant OM; the lower the value the more decomposed is the peat) load negatively in $_{IR}$Cp1, and

Table 2. Correlation between the principal components ($_{PY}$Cp1–$_{PY}$Cp3) synthesizing the molecular composition of the peat OM and the extracted FTIR components ($_{IR}$Cp1–$_{IR}$Cp5 and detrended $_{IR}$Cp1–d_{IR}Cp1), for the section containing the HPAE (300–460 cm depth).

	$_{PY}$Cp1	$_{PY}$Cp2	$_{PY}$Cp3
$_{IR}$Cp1	0.95	−0.05	−0.10
$_{IR}$Cp2	−0.02	0.68	0.58
$_{IR}$Cp3	0.85	0.18	0.19
$_{IR}$Cp5	−0.86	0.28	−0.13
$d_{_IR}$Cp1	0.89	0.18	0.00

they are usually used as peat decomposition proxies (Broder *et al.* 2012; Biester *et al.* 2014; Kylander *et al.* 2018). On the other hand, a higher degree of decomposition implies higher aromaticity (IR_3 and IR_7) and a predominance of shorter length/higher branching aliphatics (IR_5). The abundance of O-rich compounds (IR_6) decreases with decomposition (negative loading in $_{IR}$Cp1) but increases with increased organic acids content and decreased proteinaceous compounds ($_{IR}$Cp3). The predominance of guaiacol over syringol lignin moieties (IR_8) is only partially related to decomposition, but most of its variation is not captured by the PCA components.

Chronology of changes in peat organic matter composition

Based on the extracted FTIR-PCA components and FTIR ratios, we describe below the chronology of changes in OM composition in the Store Mosse peat sequence (Fig. 7). The FTIR ratios that are highly correlated to peat decomposition ($_{IR}$Cp1) are not discussed further to avoid redundancy. As already indicated, the set of records described so far reflects the presence of long-term (i.e. peat age dependent) and short-term (i.e. peat age independent) changes in the evolution of peat OM in Store Mosse; and interpretation that is in line with previous studies performed on long peat sequences (Kuhry & Vitt 1996; Malmer & Wallén 1999; Cocozza *et al.* 2003; Zaccone *et al.* 2007, 2011; Broder *et al.* 2012; Krumins *et al.* 2012; Silamikele *et al.* 2012; Biester *et al.* 2014).

Long-term changes in peat OM

$_{IR}$Cp1 is the only component showing a whole-sequence correlation to peat age (Table 3), which is slightly non-linear ($r = 0.87$ fitting a quadratic function). This indicates that up to 76% of the change in the major peat components (i.e. polysaccharides, lignin and aliphatics) is related to long-term peat decomposition. The trend is not as obvious in the bog stage but is significant in the fen peat (Table 3). As expected, the same process is reflected by the IR ratios related to the degree of peat decomposition (IR_1 and IR_2; Table 3), with the negative correlation indicating enrichment in aromatics and aliphatics and depletion of polysaccharides. The ageing of the peat also results in higher aromaticity and lower aliphaticity (IR_3, IR_4 and IR_7; Table 3), lower content in organic acids (IR_6) and higher content of guaiacol vs. syringol lignin moieties (IR_8).

Our data thus indicate that the increase in aromaticity is accompanied by an increase in G/S ratio (guaiacol/syringol). Using Py-GC-MS, Schellekens *et al.* (2015) investigated a peat sequence from a graminoid-dominated peatland and found that lignin decomposition was more complex than expected. Depending on structural composition (i.e. side chains), lignin showed no correlation to short-term changes in bog hydrology (moieties with C_3 alkyl), dependence on dry or wet conditions (acetyl moieties), source vegetation (vanillic and syringic acid) or stage of decay (depletion of G over S moieties under dry conditions). Studies on the molecular composition of peat have already shown that syringyl groups in lignin are more susceptible to degradation, while recent work suggests that biomass recalcitrance is correlated to lignin structure and that an increase in S lignin results in reduced biomass cell wall recalcitrance (Li *et al.* 2016). These authors also found that lignins from herbaceous plants had relatively less inhibition potential on biodegradation than those of woody biomass, pointing to a relevant role of source vegetation in lignin preservation. Limited biochemical activity in bogs may also contribute to the preservation of lignin and lignin-like structures (Mascarenhas *et al.* 2000).

Except for $_{IR}$Cp2 (alkynes/N compounds), the other principal components show age-dependency either in the fen ($_{IR}$Cp5) or the bog ($_{IR}$Cp3, $_{IR}$Cp4) section. Aliphatics have a secondary enrichment ($_{IR}$Cp5) with age in the fen peat, while in the bog peat carboxylates ($_{IR}$Cp3) tend to decrease and proteinaceous compounds ($_{IR}$Cp3) tend to increase with peat age. The increase in aromaticity ($_{IR}$Cp1 IR_3 and IR_7) is, again, more pronounced in the fen peat and the depletion in oxygen-rich compounds (IR_6) in the bog peat (Table 3). The shortening in chain length/increase in degree of branching of aliphatics (negative correlation with IR_5, Table 3) seems to be age-dependent to some extent, probably because the aliphatic signal in the fen peat is mostly from lipidic structures (long-chain compounds), whereas the bog peat has a significant contribution of short-chains in lignin. These results indicate that the type of peat also plays a significant role in the long-term changes in OM composition, which may agree with the larger compositional variability found in fens when compared to bogs (Heller *et al.* 2015).

Regarding the carbonyl signal, Cocozza *et al.* (2003) and Zaccone *et al.* (2007, 2011) found a decrease in the 1735–1725 cm^{-1} absorbances with depth while the absorbance at 1710 cm^{-1} increased, and interpreted this as the result of oxidative processes leading to the release of organic acids and low molecular weight compounds. Hodgkins *et al.* (2014) follow a similar reasoning to explain the weakening of the 1720 cm^{-1} band intensity in a thaw gradient in permafrost peat, suggesting that the higher pH in fens may enhance peat decomposition and lead to a higher production of carboxylic groups. In contrast, Heller *et al.* (2015) found no such increase with depth. At Store Mosse the carbonyl functionalities do not show a simple trend with age/depth. On the one hand, this signal (1760–1720 cm^{-1}) is associated with $_{IR}$Cp3, showing a significant decreasing trend in the bog peat (Table 3), but not in the fen. On the other hand, the variation of carboxylates (1709 cm^{-1}) is split between

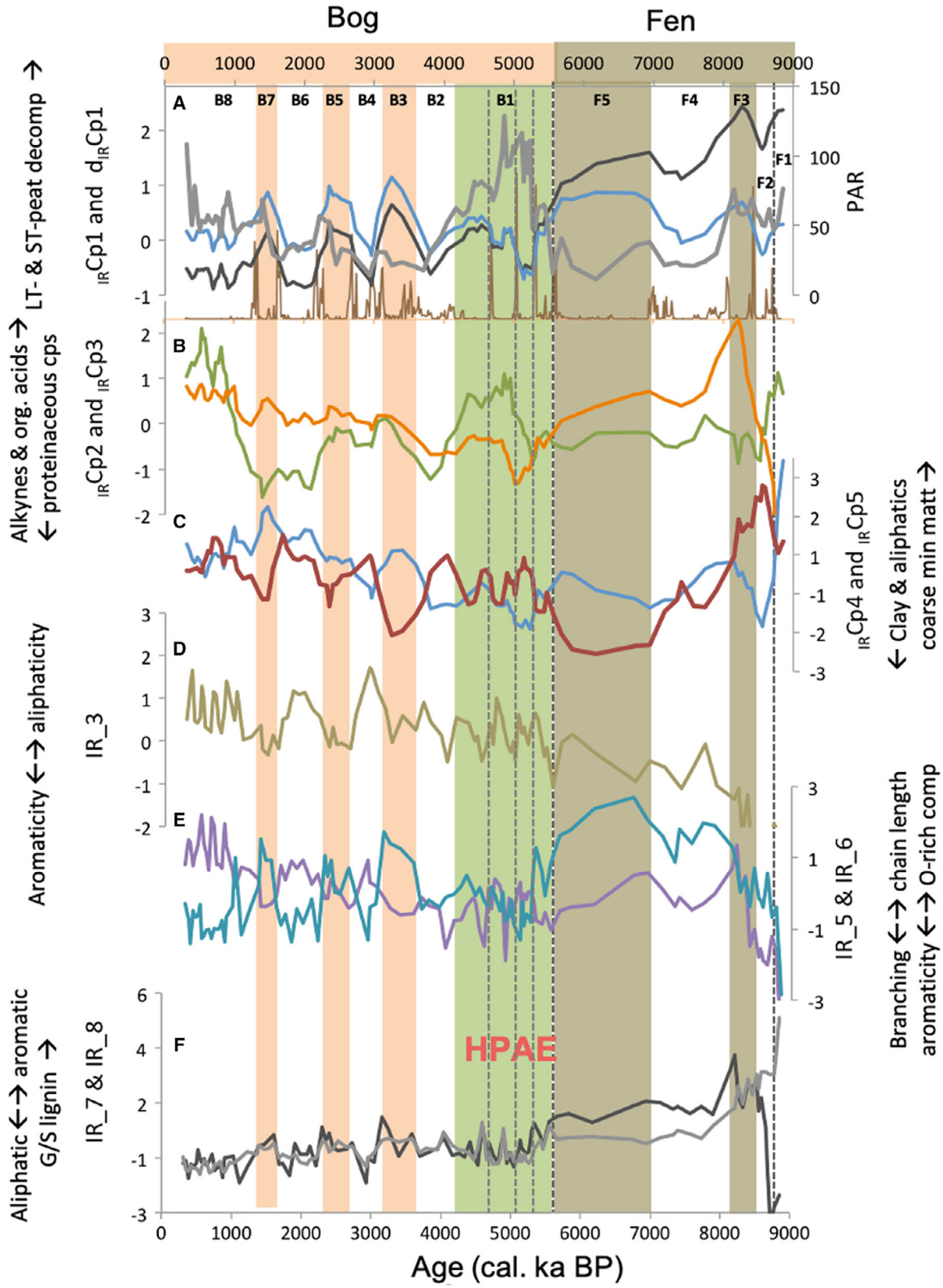

Fig. 7. Chronology of changes in Store Mosse peat organic matter composition. A. LT-decom = long-term peat decomposition ($_{IR}$Cp1, black); ST-decomp = short-term peat decomposition (d_{IR}Cp1, blue); peat accumulation rate (PAR; grey); probability of change-point (brown). B. $_{IR}$Cp2 (green) and $_{IR}$Cp3 (orange). C. $_{IR}$Cp5 (red). D. IR_3 (z-scores). E. IR_5 (z-scores, light brown) and IR_6 (z-scores, purple). F. IR_7 (z-scores, black) and IR_8 (z-scores, grey). F1 to F5 = phases of OM change in the fen stage; B1 to B8 = phases of change in OM in the bog stage. HPAE = high peat accumulation event (green shadow); brown areas are phases of higher decomposition (fen: dark; bog: light).

Table 3. Correlation between peat age and the FTIR-PCA components and FTIR ratios (IR_2 is not included as it is highly correlated to IR_1 and basically provides the same information).

	N	Cp1	Cp2	Cp3	Cp5	IR_1	IR_3	IR_4	IR_5	IR_6	IR_7	IR_8
Whole core	105	0.82	−0.18	−0.26	0.05	−0.83	−0.78	0.71	0.37	−0.65	0.76	0.78
Fen	24	0.71	0.28	−0.27	0.82	−0.38	−0.85	0.34	−0.74	−0.45	0.80	0.43
Bog	81	0.43	−0.21	−0.84	−0.36	−0.56	−0.42	0.32	0.26	−0.75	0.46	0.42

$_{IR}$Cp3 and $_{IR}$Cp1. $_{IR}$Cp1 is more expressed in the fen peat than in the bog peat, which suggests that decomposition of fen peat increases the production of carboxylates but that bog peat inhibits it. Possibly, this is due to the greater biochemical activity in minerotrophic than in ombrotrophic environments (Heller *et al.* 2015).

Short-term changes in peat OM

Change-point modelling was applied to the short-term decomposition (d_{IR}Cp1) record to objectively identify significant changes and determine the main phases of time-independent variations in peat OM. This resulted in the detection of five phases in the fen (F1–F5, Fig. 7) and eight in the bog stages (B1–B8), including the high peat accumulation event (B1, HPAE).

Fen section (~9.0 to ~5.8 cal. ka BP): minerotrophic peat. – Overall, the peat of this section has the highest degree of decomposition ($_{IR}$Cp1), low alkyne/N compounds content ($_{IR}$Cp3), high content of organic acids/carboxylic groups ($_{IR}$Cp3) and relatively high aliphatic content ($_{IR}$Cp5). Observed aromaticity is the highest of the sequence (IR_3 and IR_7), with a predominance of guaiacol over syringol lignin moieties (IR_8). Despite these general OM properties, change-point modelling identifies five main phases of change in peat decomposition in this section (Fig. 7).

Phases F1 (>~8.7 ka), F2 (~8.7–8.4 ka), and F4 (~8.1–7.0 ka) are characterized by relatively lower degree of peat decomposition (d_{IR}Cp1), with F2 having the lowest. F1 shows high alkyne/N compounds content ($_{IR}$Cp2), very low organic acids/carboxylates ($_{IR}$Cp3), shorter chain length (or more branched) aliphatics (IR_5), and O-rich compounds (IR_6), but very high aromaticity (IR_7) and syringol over guaiacol moieties (IR_8). F2 is mainly characterized by an increase in aromaticity and aliphatic chain length and decrease in alkynes/N compounds. F4 is characterized by a moderate increase in aliphatics.

Phases F3 (~8.4–8.1 ka) and F5 (~7.0–5.8 ka) are characterized by relatively higher degree of peat decomposition. F3 corresponds to the 8.2 ka event and shows a large increase in organic acids/carboxylates and aromatics, and predominance of guaiacol over syringol lignin moieties. F5 shows the highest content of long-chain aliphatics, elevated aromaticity and predominance of guaiacyl over syringyl lignin.

Bog section (~5.8 cal. ka BP to present): ombrotrophic peat. – By ~5.8 ka Store Mosse initiated a rapid transition (~200 years) from fen to bog, shortly after followed by the high peat accumulation event with the onset by ~5.5 ka (HPAE, B1). This fen–bog transition and then HPAE is shown by a large decrease in peat decomposition (Fig. 7), accompanied by elevated proportions of polysaccharides, 4-vinylphenol and 4-isopropenylphenol in the molecular compositional data. Because decomposition of the source of these compounds is known to occur under aerobic conditions (Schellekens *et al.* 2015), this indicates that, during the HPAE, bog surface wetness was high because of increased precipitation and/or rapid peat growth (faster incorporation of peat into the anaerobic catotelm). However, after having reached the highest peat accumulation rate and lowest decomposition (by ~4.7 ka), drier conditions may have also favoured the advance of heather. This is confirmed by macrofossil analyses conducted on a more recently collected sequence (in 2018), which was taken at a location proximal (within 10s of metres) to the 2008 coring location (Ryberg *et al.* 2019; Fig. S4) and is consistent with the increase in lignin in the second part of the HPAE. Lignin would increase due to the heather wood input, and because lignin of woody plants is more resistant to degradation than that of herbaceous vegetation (Li *et al.* 2016).

As revealed by change-point modelling, the HPAE exhibits internal structure and is composed of four sub-phases (Fig. 7). The first sub-phase (~5.5–5.3 ka) marks the onset of slowing decomposition rates and increasing accumulation rates and is associated with the shift from *Eriophorum* to *Sphagnum* dominated peat. The second sub-phase (~5.3–5.0 ka) shows an accelerated decrease in peat decomposition and in organic acids (carbonyl structures) and coincides with the extraordinarily high accumulation rates of the HPAE (Kylander *et al.* 2018). The last two sub-phases (~5.0–4.7 and ~4.7–4.1 ka) represent a step increase in peat decomposition, organic acids, and alkynes/N compounds – which remain elevated for the rest of the HPAE. These phases are mirrored in the mineral dusts deposited at this time (Kylander *et al.* 2016, 2018). Geochemical ratios indicated a shift to deposition

of nutrient-rich minerals during the HPAE, relatively enriched in P, K and Ca, suggested to have fertilized the bog and contributed to the elevated growth (Kylander *et al.* 2016, 2018). By ~4.7 ka BP the deposition of nutrient-rich minerals tails off.

The last ~4.0 ka of the sequence show a remarkable pattern of alternating periods of higher (B3 ~3.5–3.1 ka, B5 ~2.7–2.1 ka and B7 ~1.6–1.3 ka) and lower peat decomposition (Fig. 7). Periods of higher decomposition see an overall increase in aromaticity, with a higher guaiacol over syringol ratio of lignin (i.e. selective degradation of syringol moieties), and slight enrichment in organic acids/carboxylates. In two peatlands from the Harz Mountains (Germany), Biester *et al.* (2014) found depletion of polysaccharides and phenols and enrichment in aliphatics during drier periods due to enhanced aerobic decomposition. Although lignin and other aromatics also increased, their variation was lower than that observed for aliphatics. They argued that this might be due to the fact that changes in wetness are usually accompanied by changes in vegetation, as also suggested by Schellekens *et al.* (2015). In drier periods, woody vegetation may spread onto the mire enriching the peat in lignin products but also influencing the abundance of humic substances (Chambers *et al.* 1977; Yeloff & Mauquoy 2006).

During low-decomposition periods, lower aromaticity, slightly lower organic acid/carboxylate contents, increase in chain length/decrease in branched aliphatics and lower G/S ratios are observed, consistent with what has been observed here.

Connections to climate change

The record of short-term decomposition (i.e. time-detrended $_{IR}$Cp1 scores, d$_{IR}$Cp1) at Store Mosse is plotted in Fig. 8. The dry and cold Holocene periods reconstructed by Wanner *et al.* (2011) are also included. As described, overall peat decomposition ($_{IR}$Cp1) is higher in the fen than in the bog section. Five main phases of increased decomposition were found in Store Mosse: F3 (~8.4–8.1 ka, assigned to the 8.2 ka event) and F5 (~8.1–5.6 ka) in the fen stage, as well as B3 (~3.5–3.1 ka), B5 (~2.7–2.1 ka) and B7 (~1.6–1.3 ka) in the bog stage. Although dry and cold conditions are coeval for most of the Holocene, the peat decomposition record of Store Mosse seems to be better in phase with dry periods; four of the five events match with major periods of increased dryness. B5 (~2.7–2.1 ka) is notably the only one that does not fit, i.e. there is no correlative increase in dryness but it is coeval with a major cold episode (Fig. 7). Within the uncertainty of the age model, this period can be correlated to the 2.8 ka event, which is generally considered as a cold phase in the Northern Hemisphere, but whether it was wet or dry is still under debate (Wanner *et al.* 2011). At least for southern Scandinavia, the Store Mosse record suggests it may have been largely wet.

The HPAE (B1, ~5.6–4.1 ka) is a remarkable feature in the evolution of Store Mosse. The low peat decomposition and increased peat growth are coeval with a long period of low dryness values, and its internal structure might have been determined by

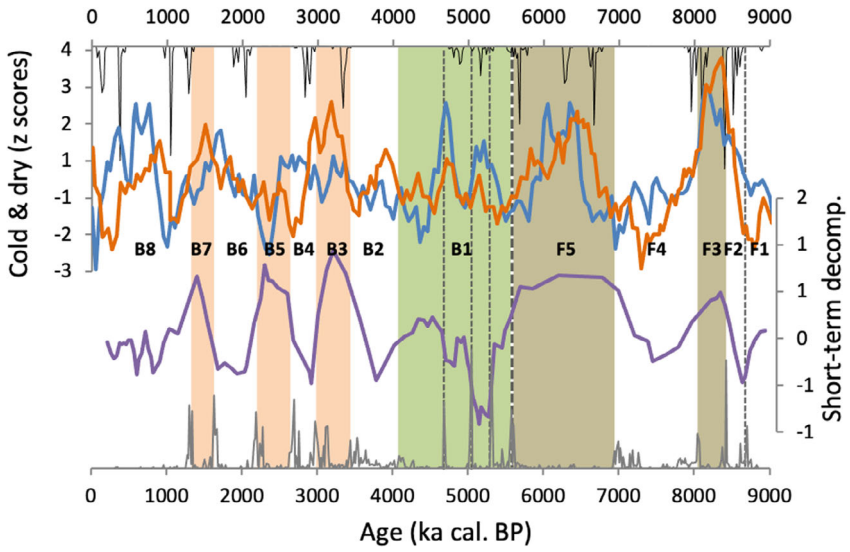

Fig. 8. Top: Holocene dry (orange) and cold (blue) phases (after Wanner *et al.* 2011); the thin black line is the probability of a change-point in the dryness record. Bottom: short-term peat decomposition (age-detrended $_{IR}$Cp1); the thin grey line is the probability of a change-point. F1 to B8 = peat decomposition phases – see text. The green area corresponds to the HPAE, and brown areas are phases of higher decomposition (fen: dark; bog: light).

two short cold and dry spells (Fig. 8). This internal structure correlates rather well with the variations in peat accumulation and C/N and inorganic geochemistry that have been discussed in previous investigations (Kylander *et al.* 2016, 2018).

Conclusions

In this study, we used vibrational spectroscopy (FTIR) to investigate the molecular composition of the organic matter of the peat and related its changes to bog responses to environmental drivers. The spectra enabled us to identify vibrations pertaining to the main constituents of the peat (polysaccharides, aliphatics, aromatics, nitrogen compounds, etc.), but also of some other minor components (such as alkynes).

The compositional differences that were found mainly relate to the type of peat (fen or bog peat) and degree of peat decomposition. On average, fen peat showed lower absorbances of polysaccharides and higher absorbances of aliphatics and carboxylates, while the opposite was found for bog peat. However, both types showed a certain degree of variability: aromatics and polysaccharides (1300–1100 cm^{-1}), carboxylates and nitrogen compounds (1800–1660 cm^{-1}) and aliphatics (3000–2800 cm^{-1}) in the fen peat, and polysaccharides (1000–900 cm^{-1}), aliphatics (1464 cm^{-1}), aromatics and nitrogen compounds (1600–1550 cm^{-1}), alkynes (2190–1960 cm^{-1}), and OH vibrations (3400–3200 cm^{-1}) in the bog peat.

Superimposed on the effects of the type of peat are the changes imposed by peat decomposition. Peat decomposition showed two main patterns: a long-term and short-term trend. While the former is highly correlated to peat age, due to the slow decomposition of peat with time, the shorter-term decomposition seems to have been driven by the conditions prevailing when the peat was at the surface of the mire. But, as exemplified by the HPAE (~5.6–3.9 ka) the long-term Store Mosse record also captures particular events in the mire's evolution. Consistent with previous investigations (by Py-GC-MS and plant macrofossil data), the FTIR results point to a rapid decrease in peat decomposition (i.e. increase in polysaccharides and decrease in aromatic and aliphatic functionalities). The results also suggest that the event had internal structure, with two sub-phases of accelerated decrease in peat decomposition. One of the particularities of the HPAE is the prominent signal of the alkynes, which are also elevated in the basal (i.e. peat inception) and the upper part (i.e. present-day acrotelm) of the peat sequence, probably related to enhanced mire bioproductivity – which may deserve further investigation.

A comparison to Holocene climate records for the Northern Hemisphere points to climate-induced changes in the mire's hydrology, affecting peat decomposition. Increased decomposition is coeval with dry periods, when the water table may have been low and oxygen availability higher. Nevertheless, changes in bog hydrology would be expected to also affect vegetation composition, which may induce chemical change in the peat. At this stage this effect is still largely unknown for Store Mosse and further investigation on the correlation between peat molecular composition and plant macrofossil records is warranted.

Short or low-resolution peat sequences may not capture all of the complexities driving peat OM compositional change; an important aspect to understand in order to project how future climate changes will affect peatlands. The systematic use of spectroscopic analyses on high-resolution peat sequences, covering temporally long periods (i.e. Holocene), combined with more sophisticated statistical methods (such as partial least squares and structural equation modelling), may help to understand the response of peatlands to past climate changes, palaeohydrology in particular.

Acknowledgements. – The County of Jönköping is thanked for providing the opportunity to sample in Store Mosse National Park, and also Stiftelsen Anna och Gunnar Vidfelts fond för biologisk forskning who provided support for the 2008 fieldwork. Sarah Greenwood is gratefully acknowledged for her help in making the soil coverage map and modelled extent of Lake Fornbolmen in Figure 1. This research has been partially funded by Consiliencia network (ED 431D2017/08) Xunta de Galicia, GPC (ED431B 2018/20) Xunta de Galicia. We thank Bjorn Robroek and an anonymous reviewer for their comments and suggestions, which helped to improve the original manuscript.

Author contributions. – Conceptualization: AMC, JKS, MEK, RB; peat analyses: OLC, MEK, JKS, EER, JK; statistical analysis: AMC, NAF; funding acquisition: MEK, AMC, OLC; writing, reviewing and editing: AMC, JKS, EER, MEK, JK, OLC, NAF, RB.

Data availability statement. – The data used in this manuscript (standardized absorbances of the selected peaks) will be available at the Bolin Center database repository (https://bolin.su.se/data/martinez-cortizas-2021-store-mosse).

References

Álvarez Fernández, N. & Martínez Cortizas, A. 2020: *andurinha: make spectroscopic data processing easier*. R package version 0.0.2. https://CRAN.R-project.org/package_andurinha.

Artz, R. R. E., Chapman, S. J. & Campbell, C. D. 2006: Substrate utilisation profiles of microbial communities in peat are depth dependent and correlate with whole soil FTIR profiles. *Soil Biology & Biochemistry 38*, 2958–2962.

Artz, R. R. E., Chapman, S. J., Robertson, A. H. J., Potts, J. M., Laggoun-Défarge, F., Gogo, S., Comont, L., Disnar, J.-R. & Francez, A.-J. 2008: FT-IR spectroscopy can be used as a screening tool for organic matter quality in regenerating cutover peatlands. *Soil Biology & Biochemistry 40*, 515–527.

Asapo, E. S. & Coles, C. A. 2012: Characterization and comparison of saprist and fibrist Newfoundland sphagnum peat soils. *Journal of Minerals Characterization and Engineering 11*, 709–718.

Bader, C., Müller, M., Schulin, R. & Leifeld, J. 2017: Peat decomposability in managed organic soils in relation to land-use, organic matter composition and temperature. *Biogeosciences Discussion 15*, 703–719.

Belyea, L. R. & Malmer, N. 2004: Carbon sequestration in peatland: patterns and mechanisms of response to climate change. *Global Change Biology 10*, 1043–1052.

Biester, H., Knorr, K.-H., Schellekens, J., Basler, A. & Hermanns, Y.-M. 2014: Comparison of different methods to determine the degree of peat decomposition in peat bogs. *Biogeosciences 11*, 2691–2707.

Bindler, R. 2003: Estimating the natural background atmospheric deposition rate of mercury utilizing ombrotrophic bogs in south Sweden. *Environmental Science and Technology 37*, 40–46.

Bindler, R., Brännvall, M.-L., Renberg, I., Emteryd, O. & Grip, H. 1999: Natural lead concentrations in pristine boreal forest soils and past pollution trends: a reference for critical load models. *Environmental Science and Technology 33*, 3362–3367.

Bindler, R., Klarqvist, M., Klaminder, J. & Forster, J. 2004: Does within-bog spatial variability of mercury and lead constrain reconstructions of absolute deposition rates from single peat records? The example of Store Mosse, Sweden. *Global Biogeochemical Cycles 18*, GB3020, https://doi.org/10.1029/2004GB002270.

Bjermo, T. 2019: *Eoliska avlagringar och vindriktningar under holocen i och kring Store Mosse, södra Sverige*. B.Sc. Candidate Project Thesis, Lund University, 62 pp.

Blaauw, M. & Christen, J. A. 2011: Flexible paleoclimate age-depth models using an autoregressive gamma process. *Bayesian Analysis 6*, 457–474.

Bourdon, S., Laggoun-Defarge, F., Disnar, J. R., Maman, O., Guillet, B., Derenne, S. & Largeau, C. 2000: Organic matter sources and early diagenetic degradation in a tropical peaty marsh (Tritrivakely, Madagascar). Implications for environmental reconstruction during the Sub-Atlantic. *Organic Geochemistry 31*, 421–438.

Broder, T., Blodau, C., Biester, H. & Knorr, K. H. 2012: Peat decomposition records in three pristine ombrotrophic bogs in southern Patagonia. *Biogeosciences 9*, 1479–1491.

Buurman, P., Nierop, K. G. J., Pontevedra-Pombal, X. & Martínez Cortizas, A. 2006: Molecular chemistry by pyrolysis–GC/MS of selected samples of the Penido Vello peat deposit, Galicia, NW Spain. *Developments in Earth Surface Processes 9*, 217–240.

Chambers, F. M., Barber, K. E., Maddy, D. & Brew, J. 1977: A 5500-year proxy-climate and vegetation record from blanket mire at Talla Moss, Borders, Scotland. *The Holocene 7*, 391–399.

Chang, C. W., Laird, D. A., Mausbach, M. J. & Hurburgh Jr, C. R. 2001: Near-infrared reflectance spectroscopy - principal components regression analysis of soil properties. *Soil Science Society of America Journal 65*, 480–490.

Chapman, S. J., Campbell, C. D., Fraser, A. R. & Puri, G. 2001: FT-IR spectroscopy of peat in and bordering Scots pine woodland: relationship with chemical and biological properties. *Soil Biology & Biochemistry 33*, 1193–1200.

Coates, J. 2000: Interpretation of infrared spectra, a practical approach. *In* Meyers, R. A. (ed.): *Encyclopedia of Analytical Chemistry*, 10815–10837, John Wiley & Sons Ltd, Chichester.

Cocozza, D., D'Orazio, V., Miano, T. M. & Shotyk, W. 2003: Characterization of solid and aqueous phases of a peat bog profile using molecular fluorescence spectroscopy, ESR and FT-IR, and comparison with physical properties. *Organic Geochemistry 34*, 49–60.

Dommain, R., Couwenberg, J. & Joosten, H. 2011: Development and carbon sequestration of tropical peat domes in south-east Asia: links to post-glacial sea-level changes and Holocene climate variability. *Quaternary Science Review 30*, 999–1010.

Edvardsson, J., Linderson, H., Rundgren, M. & Hammarlund, D. 2012: Holocene peatland development and hydrological variability inferred from bog-pine dendrochronology and peat stratigraphy – a case study from southern Sweden. *Journal of Quaternary Science 27*, 553–563.

Ellerbrock, R. H. & Gerke, H. H. 2004: Characterizing organic matter of soil aggregate coatings and biopores by Fourier transform infrared spectroscopy. *European Journal of Soil Science 55*, 219–228.

Estracanholli, E. S., Nicolodelli, G., Pratavieira, S., Kurachi, C. & Bagnato, V. S. 2012: Mathematical methods to analyze spectroscopic data – new applications. *In* Farrukh, M. A. (ed.): *Advanced Aspects of Spectroscopy*, 483-498. IntechOpen, London. http://dx.doi.org/10.5772/48318

Fernández-Getino, A. P., Hernandez, Z., Piedra Buena, A. & Almendros, G. 2013: Exploratory analysis of the structural variability of forest soil humic acids based on multivariate processing of infrared spectral data. *European Journal of Soil Science 64*, 66–79.

Gallagher, K., Bodin, T., Sambridge, M., Weiss, D., Kylander, M. & Large, D. 2011: Inference of abrupt changes in noisy geochemical records using transdimensional changepoint models. *Earth and Planetary Science Letters 311*, 182–194.

Granlund, E. 1932: De svenska Hogmossarnas geologi. *Sveriges Geologiska Undersökning 26*, 1–93.

Griffiths, P. R. & De Haseth, J. A. 2007: *Fourier Transform Infrared Spectrometry*. 560 pp. John Wiley & Sons, Chichester.

Haberhauer, G. & Gerzabek, M. H. 1999: Drift and transmission FT-IR spectroscopy of forest soils: an approach to determine decomposition processes of forest litter. *Vibrational Spectroscopy 19*, 413–417.

Haberhauer, G., Feigl, B., Gerzabek, M. H. & Cerri, C. 2000: FT-IR spectroscopy of organic matter in tropical soils: changes induced through deforestation. *Applied Spectroscopy 54*, 221–224.

Haberhauer, G., Rafferty, B., Strebl, F. & Gerzabek, M. H. 1998: Comparison of the composition of forest soil litter derived from three different sites at various decompositional stages using FTIR spectroscopy. *Geoderma 83*, 331–342.

Hansson, S. V., Kaste, J. M., Chen, K. & Bindler, R. 2014: Beryllium-7 as a natural tracer for short-term downwash in peat. *Biogeochemistry 119*, 329–339.

Hansson, S. V., Rydberg, J., Kylander, M., Gallagher, K. & Bindler, R. 2013: Evaluating paleoproxies for peat decomposition and their relationship to peat geochemistry. *The Holocene 23*, 1666–1671.

Heller, C., Ellerbrock, R. H., Roskopf, N., Klingenfus, C. & Zeitz, J. 2015: Soil organic matter characterization of temperate peatland soil with FTIR-spectroscopy: effects of mire type and drainage intensity. *European Journal of Soil Science 66*, 847–858.

Hodgkins, S. B., Richardson, C. J., Dommain, R., Wang, H., Glaser, P. H., Verbeke, B., Winkler, B. R., Cobb, A. R., Rich, V. I., Missilmani, M., Flanagan, N., Ho, M., Hoyt, A. M., Harvery, C. F., Vining, S. R., Hough, M. A., Moore, T. R., Richard, P. J., De la Cruz, F. B., Toufaily, J., Hamdan, R., Cooper, W. T. & Chanton, J. P. 2018: Tropical peatland carbon storage linked to global latitudinal trends in peat recalcitrance. *Nature Communications 9*, 3640, https://doi.org/10.1038/s41467-018-06050-2.

Hodgkins, S. B., Tfaily, M. M., McCalley, C. K., Logan, T. A., Crill, P. M., Saleska, S. R., Rich, V. I. & Chanton, J. P. 2014: Changes in peat chemistry associated with permafrost thaw increase greenhouse gas production. *Proceedings of the National Academy of the United States of America 111*, 5819–5824.

Holmgren, A. & Nordén, B. 1988: Characterization of peat samples by diffuse reflectance FT-IR spectroscopy. *Applied Spectroscopy 2*, 255–262.

Janik, L. J., Skjemstad, J., Shepherd, K. & Spouncer, L. 2007: The prediction of soil carbon fractions using mid-infrared-partial least square analysis. *Australian Journal of Soil Research 45*, 73–81.

Kaal, J., Baldock, J. A., Buurman, P., Nierop, K. G. J., Pontevedra-Pombal, X. & Martínez-Cortizas, A. 2007: Evaluating pyrolysis–GC/MS and 13C CPMAS NMR in conjunction with a molecular mixing model of the Penido Vello peat deposit, NW Spain. *Organic Geochemistry 38*, 1097–1111.

Kalbitz, K., Geyer, W. & Geyer, S. 1999: Spectroscopic properties of dissolved humic substances – a reflection of land use history in a fen. *Biogeochemistry 47*, 219–238.

Klavins, M. & Purnalis, O. 2014: Characterization of humic acids from raised bog peat. *Latvian Journal of Chemistry 1*, 83–97.

Krumins, J., Klavins, M. & Seglins, V. 2012: Comparative study of peat composition by using FT-IR spectroscopy. *Material Science and Applied Chemistry 26*, 106–114.

Kuhry, P. & Vitt, D. H. 1996: Fossil carbon/nitrogen ratios as a measure of peat decomposition. *Ecology 77*, 271–275.

Kylander, M. E., Bindler, B., Martínez Cortizas, A., Gallagher, K., Mörth, C.-M. & Rauch, S. 2013: A novel geochemical approach to paleorecords of dust deposition and effective humidity: 8500 years of peat accumulation at Store Mosse (the "Great Bog"), Sweden. *Quaternary Science Reviews 69*, 69–82.

Kylander, M. E., Martínez-Cortizas, A., Bindler, R., Greenwood, S. L., Mörth, C.-M. & Rauch, S. 2016: Potentials and problems of building detailed dust records using peat archives: an example from Store Mosse (the "Great Bog"), Sweden. *Geochimica et Cosmochimica Acta 190*, 156–174.

Kylander, M., Martínez-Cortizas, A., Bindler, R., Kaal, J., Sjöström, J. K., Hansson, S. V., Slva-Sánchez, N., Greenwood, S., Hallagher, K., Rydberg, J., Mörth, C.-M. & Racuh, S. 2018: Mineral dust as a driver of carbon accumulation in northern latitudes. *Scientific Reports 8*, 6876, https://doi.org/10.1038/s41598-018-25162-9.

Larkin, P. J. 2011: *IR and Raman Spectroscopy, Principles and Spectral Interpretation*. 228 pp. Elsevier, Amsterdam.

Li, M., Pu, Y. & Ragauskas, A. J. 2016: Current understanding of the correlation of lignin structure with biomass recalcitrance. *Frontiers in Chemistry 4*, 45, https://doi.org/10.3389/fchem.2016.00045.

Loisel, J. & 60 others. 2014: A database and synthesis of northern peatland soil properties and Holocene carbon and nitrogen accumulation. *The Holocene 24*, 1028–1042.

Lundqvist, J. & Wohlfarth, B. 2001: Timing and east-west correlation of south Swedish ice marginal lines during the Late Weichselian. *Quaternary Science Reviews 20*, 1127–1148.

Malmer, N. & Wallén, B. 1999: The dynamics of peat accumulation on bogs: mass balance of hummocks and hollows and its variation throughout a millennium. *Ecography 22*, 736–750.

Malmer, N. & Wallen, B. 2004: Input rates, decay losses and accumulation rates of carbon in bogs during the last millennium: internal processes and environmental changes. *The Holocene 14*, 111–117.

Malmer, N., Svensson, G. & Wallen, B. 1997: Mass balance and nitrogen accumulation in hummocks on a South Swedish bog during the late Holocene. *Ecography 20*, 535–549.

Mascarenhas, M., Dighton, J. & Arbuckle, G. A. 2000: Characterization of plant carbohydrates and changes in leaf carbohydrate chemistry due to chemical and enzymatic degradation measured by microscopic ATR FT-IR spectroscopy. *Applied Spectroscopy 54*, 681–686.

Müller, C. M., Pejcic, B., Esteban, L., Piane, C. D., Raven, M. & Mizaikoff, B. 2014: Infrared attenuated total reflectance spectroscopy: an innovative strategy for analyzing mineral components in energy relevant systems. *Scientific Reports 4*, 6764, https://doi.org/10.1038/srep06764.

Neves Fernandes, A., Govanela, M., Esteves, V. I. & de Souza Sierra, M. M. 2010: Elemental and spectral properties of peat and soil samples and their respective humic substances. *Journal of Molecular Structure 971*, 33–38.

Niemeyer, J., Chen, Y. & Bollag, J. M. 1992: Characterization of humic acids, composts, and peat by diffuse reflectance Fourier-transform infrared spectroscopy. *Soil Science Society of America Journal 56*, 135–140.

Pérez-Rodríguez, M., Horák-Terra, I., Rodríguez-Lado, L. & Martínez Cortizas, A. 2016: Modelling mercury accumulation in minerogenic peat combining FTIR-ATR spectroscopy and partial least squares (PLS). *Spectrochimica Acta Part A: Molecular and Biomolecular Spectroscopy 168*, 65–72.

R Core Team 2020: *R: A language and environment for statistical computing*. R Foundation for Statistical Computing, Vienna, Austria. https://www.R-project.org/.

Rajalahti, T., Arneberg, R., Berven, F. S., Myhr, K.-M., Ulvik, R. J. & Kvalheim, O. 2009: Biomarker discovery in mass spectral profiles by means of selectivity ratio plot. *Chemometrics and Intelligent Laboratory Systems 95*, 35–48.

Robroek, B. J. M., Albrecht, R. J. H., Hamard, S., Pulgarin, A., Bragazza, L., Buttler, A. & Jassey, V. E. J. 2016: Peatland vascular plant functional types affect dissolved organic matter chemistry. *Plant and Soil 407*, 135–143.

Ryberg, E., Kylander, M. E., Väliranta, M. & Ehrlén, J. 2019: Temporal scale changes in species distribution in boreal peatlands: Store Mosse, south-central Sweden (preliminary results) (Poster session). INQUA Congress 2019, Dublin, Ireland.

Schellekens, J., Bindler, R., Martínez-Cortizas, A., McClymont, E. L., Abbott, G. D., Biester, H., Pontevedra-Pombal, X. & Buurman, P. 2015: Preferential degradation of polyphenols from Sphagnum – 4-Isopropenylphenol as a proxy for past hydrological conditions in Sphagnum-dominated peat. *Geochimica et Cosmochimica Acta 150*, 74–89.

Senesi, N., Miano, T. M., Provenzano, M. R. & Brunetti, G. 1991: Characterization, differentiation, and classification of humic substances by fluorescence spectroscopy. *Soil Science 152*, 259–271.

Silamikele, I., Nikodemus, O., Kalnina, L., Purnalis, O., Sire, J. & Klavins, M. 2012: Properties of peat in ombrotrophic bogs depending on the humification process. *In* Klavins, M. (ed.): *Mires and Peat*, 71–95. University of Latvia Press, Riga.

Silva-Sánchez, N., Martínez Cortizas, A., Abel-Schaad, D., López-Sáez, J. A. & Mighall, T. 2016: Influence of climate change and human activities on the organic and inorganic composition of peat during the 'Little Ice Age' (El Payo mire, W Spain). *The Holocene 26*, 1290–1303.

Silva-Sánchez, N., Schofield, J. E., Mighall, T. M., Martínez Cortizas, A., Edwards, K. J. & Foster, I. 2015: Climate changes, lead pollution and soil erosion in south Greenland over the past 700 years. *Quaternary Research 84*, 159–173.

Simonescu, C. M. 2012: Application of FTIR spectroscopy in environmental studies. *In* Farrukh, M. A. (ed.): *Advanced Aspects of Spectroscopy*, 49–84. IntechOpen, London. http://dx.doi.org/10.5772/48331

Sjöström, J. K., Martínez Cortizas, A., Hansson, S. V., Silva Sánchez, N., Bindler, R., Rydberg, J., Mörth, C.-M., Ryberg, E. E. S. & Kylander, M. 2020: Paleodust deposition and peat accumulation rates – Bog size matters. *Chemical Geology 554*, 119795, https://doi.org/10.1016/j.chemgeo.2020.119795.

SMHI (Swedish Metrological and Hydrological Institute). 2009: *Yearly precipitation, average 1961–1990*. https://www.smhi.se/klimatdata/meteorologi/nederbord/normal–uppmatt–arsnederbord–medelvarde–1961–1990–1.4160.

Socrates, G. 2001: *Infrared and Raman Characteristic Group Frequencies, Tables and Charts*. 362 pp, John Wiley & Sons Ltd, Chichester.

Stevenson, F. J. & Goh, K. M. 1971: Infrared spectra of humic acids and related substances. *Geochimica et Cosmochimica Acta 35*, 471–483.

Svensson, G. 1988a: Bog development and environmental conditions as shown by the stratigraphy at Store Mosse mire in southern Sweden. *Boreas 17*, 89–111.

Svensson, G. 1988b: Fossil plant communities and regeneration patterns on a raised bog in southern Sweden. *Journal of Ecology 76*, 41–59.

Tfaily, M. M., Cooper, W. T., Kostra, J. E., Chanton, P. R., Schadt, C. W., Hanson, P. J., Iversen, C. M. & Chanton, J. P. 2014: Organic matter transformation in the peat column at Marcell Experimental Forest: humification and vertical stratification. *Journal of Geophysical Research: Biogeosciences 119*, 661–675.

Viscarra Rossel, R. A. & Behrens, T. 2010: Using data mining to model and interpret soil diffuse reflectance spectra. *Geoderma 158*, 46–54.

Wanner, H., Solomina, O., Grosjean, M., Ritz, S. P. & Jetel, M. 2011: Structure and origin of Holocene cold events. *Quaternary Science Reviews 30*, 3109–3123.

Wastegård, S., Johansson, H. & Pacheo, J. M. 2020: New major element analyses of proximal tephras from the Azores and suggested correlations with cryptotephras in North-West Europe. *Journal of Quaternary Science 35*, 114–121.

Yeloff, D. & Mauquoy, D. 2006: The influence of vegetation composition on peat humification: implications for palaeoclimatic studies. *Boreas 35*, 662–673.

Zaccone, C., Miano, T. M. & Shotyk, W. 2007: Qualitative comparison between raw peat and related humic acids in an ombrotrophic bog profile. *Organic Geochemistry 38*, 151–160.

Zaccone, C., Sanei, H., Outridge, P. M. & Miano, T. M. 2011: Studying the humification degree and evolution of peat down a Holocene bog

profile (Inuvik, NW Canada): a petrological and chemical perspective. *Organic Geochemistry 42*, 399–408.

Supporting Information

Additional Supporting Information may be found in the online version of this article at http://www.boreas.dk.

Data S1. Analytical and methodological details.

Table S1. Loadings of the absorptions for the five extracted components (91% of the total variance; Cp1 51%, Cp2 18%, Cp3 10%, Cp4 8.0%, Cp5 4%). Highest loading for each vibration is in bold, while numbers in orange correspond to loadings implicating secondary variance allocation (10% or more of the variance of the variable). The left column corresponds to the compounds associated with the vibration.

Table S2. Correlations between FTIR ratios.

Table S3. Loadings of the compounds identified by Py-GC-MS, corresponding to the peat section of the high peat accumulation event.

Fig. S1. Age depth model of Store Mosse obtained using the Bacon routine (Blaauw & Christen 2011).

Fig. S2. Selected data from previous investigations illustrating the stratigraphy of the peat deposit. PAR = peat accumulation rates in $g\ m^{-2}\ year^{-1}$; DPH = degree of peat decomposition (standardized data). The dashed line indicates the limit between the fen (below) and the bog (above) sections.

Fig. S3. Fractionation of communalities for the absorbances used in the PCA. The different colours of the bars in the same component (Cp1, Cp3, Cp4) correspond to peaks with positive (lighter) or negative (darker) loadings

Fig. S4. Abundance of mosses and shrubs (*Erica* and *Calluna*) macro-remains in Store Mosse.